Journal of
Materials Chemistry C

REVIEW

View Article Online
View Journal | View Issue

Cite this: J. Mater. Chem. C, 2015, 3, 9496

# Arylsilanes and siloxanes as optoelectronic materials for organic light-emitting diodes (OLEDs)

Dianming Sun,[a] Zhongjie Ren,*[a] Martin R. Bryce*[b] and Shouke Yan*[a]

Received 4th June 2015,
Accepted 8th August 2015

DOI: 10.1039/c5tc01638j

www.rsc.org/MaterialsC

Organic light emitting diodes (OLEDs) are currently receiving much attention for applications in new generation full-colour flat-panel and flexible displays and as sources for low energy solid-state lighting. Arylsilanes and siloxanes have been extensively studied as components of OLEDs, mainly focusing on optimizing the physical and electronic properties of the light-emitting layer and other functional layers within the OLED architecture. Arylsilanes and siloxanes display the advantages of good solubility in common organic solvents and excellent resistance to thermal, chemical and irradiation degradations. In this review, we summarize the recent advances in the utilization of arylsilanes and siloxanes as fluorophore emitters, hosts for phosphor emitters, hole and exciton blocking materials, and as electron and hole transporting materials. Finally, perspectives and challenges related to arylsilanes and siloxanes for OLED applications are proposed based on the reported progress and our own opinions.

Open Access Article. Published on 14 augustus 2015. Downloaded on 8/10/2025 15:53:28.
This article is licensed under a Creative Commons Attribution 3.0 Unported Licence.

## 1. Introduction

In the past few decades, impressive scientific and technological progress has been achieved in the exploitation of organic light emitting diodes (OLEDs) in full-colour flat-panel displays and solid-state lighting. Since Tang *et al.*[1] reported the first OLED with one emitting layer, the device structure of OLEDs has evolved due to extensive academic and industrial efforts from a single-layer device to a multilayer structure with additional charge transporting and blocking layers to improve the device performances. Now it is well established that for realizing highly efficient OLEDs it is important for these layers to possess: (i) suitable energy levels appropriately matched with those of the neighbouring functional layers for efficient charge injection to reduce the operating voltage; (ii) balanced hole and electron transport abilities from both sides of the emitting layer to increase the recombination opportunity within the emitting layer; (iii) higher singlet or triplet energy levels than the

[a] State Key Laboratory of Chemical Resource Engineering, Beijing University of Chemical Technology, Beijing 100029, China. E-mail: skyan@mail.buct.edu.cn, renzj@mail.buct.edu.cn
[b] Department of Chemistry, University of Durham, Durham DH1 3LE, UK. E-mail: m.r.bryce@durham.ac.uk

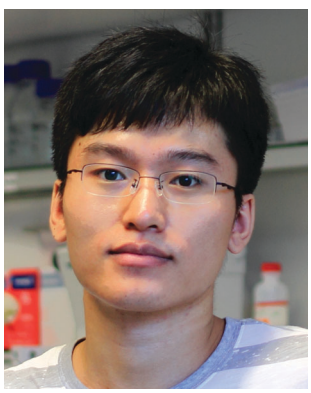

**Dianming Sun**

*Dianming Sun received his BE degree in 2011 from the college of Materials Science and Engineering at Beijing University of Chemical Technology. He is currently a PhD candidate under the supervision of Prof. Shouke Yan in the State Key Laboratory of Chemical Resource Engineering. His thesis project has focused on the development of organosilicon optoelectronic materials for phosphorescent organic light-emitting diodes.*

**Zhongjie Ren**

*Zhongjie Ren received his PhD from the State Key Laboratory of Polymer Physics and Chemistry at Institute of Chemistry, Chinese Academy of Sciences, in 2009. He then worked for two years as a postdoctoral research fellow at Beijing University of Chemical Technology. From December 2011, he was appointed as an associate professor at Beijing University of Chemical Technology. From 2014 to 2015, he moved to Durham University with Prof. Martin R. Bryce as a visiting scholar. His research interests cover the design, synthesis and application of organosilicon-based optoelectronic materials in OLEDs, resistor type memory devices and liquid crystals.*


This journal is © The Royal Society of Chemistry 2015

Open Access Article. Published on 14 augustus 2015. Downloaded on 8/10/2025 15:53:28.
This article is licensed under a Creative Commons Attribution 3.0 Unported Licence.

emitting molecules to avoid exothermic reverse energy transfer[2–4] and (iv) good thermal and morphological stabilities and film-forming abilities for longer device lifetimes. To meet these requirements the optoelectronic and physical properties of these charge transfer and blocking materials have been extensively modified through rational design of the functional substituents and chemical structures.[5–16] However, it is difficult to tune certain properties without adversely affecting others due to the close inter-relationship between optoelectronic, morphological and physical properties. For example, the thermal stability of organic materials can be enhanced by expanding their molecular size. However, additional conjugated groups may result in a decrease in solubility and changes in the intermolecular interactions in the solid state. Moreover, one may want to improve charge mobility by extending the conjugation length, while the singlet and triplet energy levels will inevitably decrease. Therefore, it is important to select materials with independent control over both the physical and optoelectronic properties. Recently, arylsilanes and siloxanes have been widely incorporated into organic optoelectronic materials to tune certain properties while maintaining others successfully.[17–82]

Arylsilanes and siloxanes belong to a class of organosilicon materials that have rich and versatile applications including anti-foaming agents, lubricants, protective coatings and microelectronics due to their good solubility, chemical and thermal stability and flexibility.[83–85] Kamino and Bender have reviewed the use of siloxanes, silsesquioxanes and silicones in organic semiconducting materials.[17] The incorporation of organosilicon groups into organic light-emitting materials has led to significant improvements, especially for those with poor thermal stabilities and high singlet or triplet energy levels. Because most organosilicon compounds used for active layers of OLEDs are dominated by bonding with aryl-substituents or oxygen atoms, this review will consider only arylsilane- and siloxane-based optoelectronic materials. Furthermore, here we broadly define arylsilanes as those materials containing tetraphenylsilane fragments, and siloxanes as those based on polyhedral oligomeric silsesquioxanes (POSS) or polysiloxanes which are often used for emitting or charge transporting layers. For examples, in 2001, Chen *et al.*[44] pioneered the use of tetraphenylsilane as the core structure for blue emitters with intrinsic large band-gaps by attaching different ratios of electron-affinity moieties. Recently, our group integrated organic functional groups with ladder polysilsesquioxanes[34] and linear polysiloxanes[43] as high triplet energy host materials for blue phosphorescent OLEDs.

In this article, we review the recent literature on arylsilanes and siloxanes which are used as emitters, charge-transport and host materials in OLEDs. The molecular structures, thermal stabilities and device performances are summarized and discussed. Specifically, the relationship between chemical structures and the properties of various organosilicon materials will be covered. Examples of hybrid materials will be discussed in detail with a focus on the specific impact of incorporating arylsilanes and siloxanes on the final physical and electronic properties of the materials. For the purpose of this article, these materials are divided into three broad groups based on the organosilicon structure and include: arylsilanes, polyhedral oligomeric silsesquioxanes and polysiloxanes. This review is written to serve as a tour of how traditional silicon chemistry can be integrated into the area of new and versatile OLED materials which are showing great promise as active components in functional devices.

## 2. High performance hybrid materials

### 2.1 Determination of the frontier molecular orbital and triplet energy levels of organic semiconductors

Over the past decades, a number of organic optoelectronic materials have been synthesized for high efficiency organic light emitting diodes. A multilayer device structure is necessary

**Martin R. Bryce**

*Martin Bryce received a BSc from Wolverhampton Polytechnic and a DPhil from York University, UK. After postdoctoral work at the Universities of British Columbia and Bristol he moved to Durham University. Since 1995 he has been a full professor of chemistry. He has held visiting scientist positions at the University of California, Santa Barbara and the University of Copenhagen. He was a Troisième Cycle Lecturer in Switzerland (2008) and Tarrant Lecturer at the University of Florida, Gainesville (2013). His research interests cover molecular design, synthesis and assembly of organic optoelectronic materials (small molecules and polymers), molecular electronics and nano-scale chemistry.*

**Shouke Yan**

*Shouke Yan received his PhD at Changchun Institute of Applied Chemistry, The Chinese Academy of Sciences (CIAC-CAS) under the joint guidance of Prof. Decai Yang and Prof. J. Petermann (Dortmund University, Germany) and then worked at Dortmund University associated with Prof. J. Petermann. In 2001, he joined the Institute of Chemistry, the Chinese Academy of Sciences as a full Professor. In 2008, he moved to Beijing University of Chemical Technology. He has obtained the Excellent Hundred Talents Award and an NSFC Outstanding Youth Fund. His current research involves surface-induced polymer crystallization, orientation-induced polymer crystallization, and phase transitions of crystalline polymers.*

Open Access Article. Published on 14 augustus 2015. Downloaded on 8/10/2025 15:53:28.
This article is licensed under a Creative Commons Attribution 3.0 Unported Licence.

to improve the overall performance. Properties such as the highest occupied molecular orbital (HOMO) and lowest unoccupied molecular orbital (LUMO) of the materials in the different layers need to be tuned appropriately for efficient charge transportation, injection and blocking. Meanwhile, besides the frontier molecular orbitals, the triplet energy levels are also important for phosphorescent OLEDs. Therefore, it is necessary to measure these properties accurately and conveniently. Accurately, the HOMO and LUMO of organic thin films can be determined by ultraviolet photoelectron spectroscopy (UPS)[86] and inverse photoelectron spectroscopy (IPES),[87] respectively. However, these experiments are complex and time consuming to reduce artificial deviation.[86] In practice, electrochemical measurements can be employed to estimate the HOMO and LUMO energies directly from the oxidation and reduction potentials which are measured with respect to a reference potential (typically the ferrocenium/ferrocene redox couple) scaled to vacuum. However, for these procedures a series of approximations are unavoidable even when all measurements are done accurately.[88] The LUMO can also be calculated by adding the optical energy gap to the HOMO energy levels, where the optical energy gap corresponds to the energy at the cut-off wavelength of the initial absorption band. It should be noted that the optical energy gap leads to an underestimation of the true energy gap between the HOMO and LUMO.[89,90] With regard to the determination of triplet energies, due to the long lifetime of the molecules in the triplet state ($10^{-4}$ to 10 s or more), the phosphorescence of organic materials has to be observed at low temperature in highly viscous media to protect the triplet state. The photoluminescence spectrum at 77 K is most commonly used for this purpose. In the following section, all HOMO and LUMO energy levels mentioned are measured by combining electrochemical measurements and absorption spectra, and triplet energy levels are determined by low temperature (77 K or lower) photoluminescence spectra, unless stated otherwise.

### 2.2 Arylsilane-based optoelectronic materials

Arylsilane derivatives belong to a series of wide bandgap materials in which the silicon atom disconnects the conjugation between each aryl unit, leading to high singlet and triplet energy levels. Meanwhile, the inherent tetrahedral configuration of arylsilanes can effectively prevent intermolecular interactions in the solid state, thereby enabling the formation of uniform and smooth amorphous films. Therefore, arylsilanes with silicon as the linkage have been widely used as core structures for ultraviolet emission, high-triplet-energy and charge-blocking materials. Moreover, different organic functional substituents can be conveniently introduced into the arylsilane framework.

Compared to green and red fluorescent emitters, there are only a few known devices fabricated from organic blue fluorescent emitters due to their intrinsic wide bandgaps.[91–93] In this context tetraphenylsilane is a good building block. For this purpose and to reduce the barrier for electron injection together with improving the thermal stability, Chen *et al.*[44] first introduced one to four triphenylaminooxadiazole (TPAOXD) electron-affinity moieties on the central tetraphenylsilane skeleton. These four blue emitters are shown in Fig. 1. The glass transition

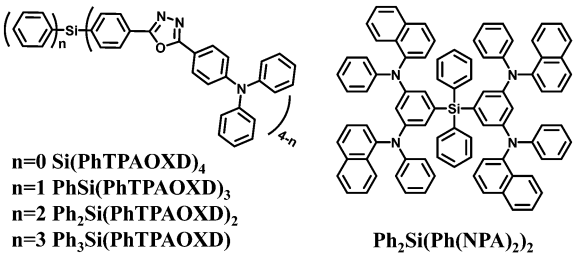


Fig. 1 Chemical structures of tetraphenylsilane derivatives functionalized with triphenylaminooxadiazole and diarylamine.

temperatures and morphological stabilities improved with increased number of TPAOXD substituents due to the larger molecular size and the stable tetraphenylsilane tetrahedral structure. Among these, $Ph_3Si$(PhTPAOXD) as the emitter in a traditional trilayer device showed the best efficiencies with brightness exceeding 20 000 cd $m^{-2}$ and a rather narrow blue emission band with Commission Internationale de l'Eclairage (CIE) coordinates of (0.17, 0.17).

Improved performance for blue OLEDs with $Ph_3Si$(PhTPAOXD)[45] (Fig. 1) as the emitter was achieved by combining the standard hole-transporting layer *N*,*N*′-bis(naphthalen-1-yl)*N*,*N*′-bis(phenyl)-benzidine (NPB) with a newly synthesized triarylamine-based tetraphenylsilane derivative bis(3,5-bis-(1-naphthylphenylamino)phenyl)-diphenylsilane ($Ph_2Si(Ph(NPA)_2)_2$) (Fig. 1). The amorphous property of $Ph_2Si(Ph(NPA)_2)_2$ in the condensed state can be attributed to the starbust nonplanar structure. The optimized device jointly using NPB and $Ph_2Si(Ph(NPA)_2)_2$ as hole-transporting layer showed a maximum electroluminescence (EL) near 19 000 cd $m^{-2}$ with reduced current density and high external quantum efficiency (EQE) of 2.4% (1.1 lm $W^{-1}$, 3.1 cd $A^{-1}$). The device possesses good blue colour purity with EL emission maximum at 460 nm, corresponding to CIE (0.16, 0.18).

However, the intrinsic low internal quantum efficiency of a fluorescent emitter such as $Ph_3Si$(PhTPAOXD) limited the application of fluorescent OLEDs. Since the pioneering work on phosphorescent OLEDs (PhOLEDs) with potential 100% internal quantum efficiency,[2] most studies have focused on developing suitable high triplet energy hosts for realizing high efficiency PhOLEDs, especially for blue phosphors.

The UGH series[46,47] (Fig. 2) were first used as host materials for blue PhOLEDs by Thompson *et al.* The ultra-high energy gap compounds, namely diphenyldi(*o*-tolyl)silane (UGH1), *p*-bis-(triphenylsilyl)benzene (UGH2), *m*-bis(triphenylsilyl)benzene (UGH3), and 9,9′-spiro-bisilaanthracene (UGH4) were employed as host for the blue phosphor bis(4′,6′-difluorophenylpyridinato)-tetrakis(1-pyrazolyl)borate (FIr6) in the emissive layer of PhOLEDs. The device structure and energy diagram are shown in Fig. 3. In addition, the high singlet (~4.0 eV) and triplet (~3.2 eV) energies associated with these materials effectively suppresses both the electron and energy transfer quenching pathways between FIr6 and the host materials, and confines the transport of both charge and excitons across the EML on the phosphor dopant, leading to deep blue devices with improved EQE

 This journal is © The Royal Society of Chemistry 2015

Open Access Article. Published on 14 augustus 2015. Downloaded on 8/10/2025 15:53:28.
This article is licensed under a Creative Commons Attribution 3.0 Unported Licence.

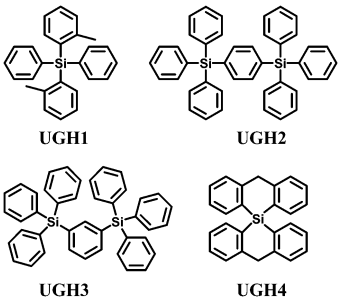


Fig. 2 Chemical structures of UGH1–4.

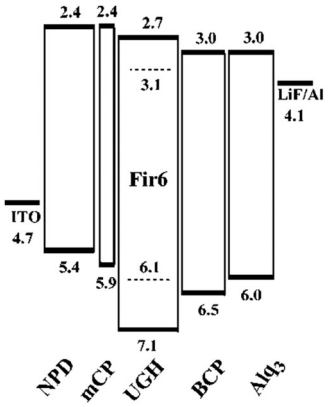


Fig. 3 The energy level diagram (units: eV) for the device: ITO/NPD (400 Å)/mCP (100 Å)/FIr6:UGH (10%, 250 Å)/BCP (150 Å)/$Alq_3$ (250 Å)/LiF/Al. Reproduced with permission from ref. 47, Copyright 2004 American Chemical Society.

compared with that of conventional systems relying on host–guest energy transfer.

However, the HOMO levels of the UGH series were estimated to be around 7.0 eV (determined by UPS[47]). Such deep HOMO levels result in inefficient hole injection from common hole transport layers. Therefore, EQE less than 10% was observed in the FIr6 doped blue PhOLEDs. In addition, the low glass transition temperatures within the range of 26–53 °C, resulted in poor thermal stability.

The increased thermal stabilities and reduced bandgap were realized by replacing the phenyl unit of UGH2 with a biphenyl or terphenyl unit, to give 4,4′-bistriphenylsilanyl-biphenyl (BSB)[57] and 4,4″-bis(triphenylsilanyl)-(1,1′,4′,1″)-terphenyl (BST)[57] with glass transition temperatures higher than 100 °C (Fig. 4). However, the triplet energies were reduced significantly (compared to UGH1–4) to 2.76 and 2.58 eV, respectively. BSB was evaluated as the best host material for the blue emitting iridium(III) bis(4,6-difluorophenylpyridinato)-4-(pyridin-2-yl)-1,2,3-triazolate (FIrpytz) dopant and a high EQE of 19.3% was obtained with CIE coordinates of (0.15, 0.32).

In general, carbazole-based derivatives are the most commonly used hosts for blue PhOLEDs due to their high triplet energy levels and good hole transport abilities. However, the electrochemically active sites (C3 and C6) can undergo chemical coupling reactions which lower the triplet energy during the device operation.

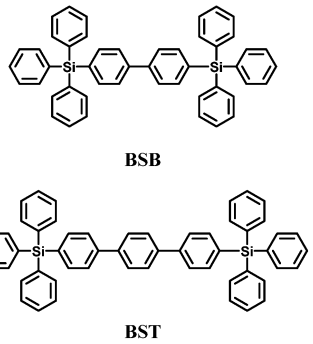


Fig. 4 Chemical structures of BSB and BST.

Bulky groups attached to C3 and C6 retain the high triplet energy of carbazole while enhancing the morphological stability by non-conjugated substitution. 3,6-Bis(triphenylsilyl)carbazole (CzSi)[52] (Fig. 5) is, therefore, an effective host material for blue electrophosphorescence with greatly enhanced morphological and electrochemical stabilities in comparison with previous carbazole-based hosts. Using CzSi, blue PhOLEDs with high efficiencies of up to EQE 16%, $\eta_{c,max}$ 30.6 cd $A^{-1}$, and $\eta_{p,max}$ 26.7 lm $W^{-1}$ were demonstrated.

Moreover, a series of tetraphenylsilanes containing different ratios of carbazoles, namely bis(4-(9-carbazolyl)phenyl)dimethylsilane (DMSiCBP),[61] bis(4-(9-carbazolyl)phenyl)diphenylsilane (DPSiCBP),[61] DCzSiCz,[70] DDCzSi[70] and DTCzSi[70] were used as

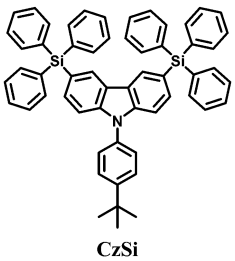


Fig. 5 Chemical structure of CzSi.

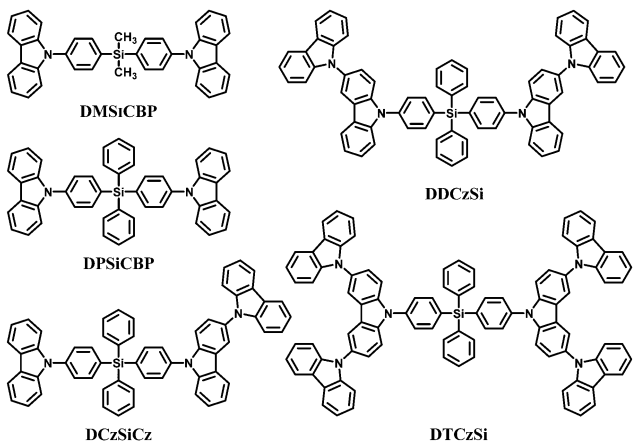


Fig. 6 Chemical structures of arylsilane derivatives functionalized with carbazole.

Open Access Article. Published on 14 augustus 2015. Downloaded on 8/10/2025 15:53:28.
This article is licensed under a Creative Commons Attribution 3.0 Unported Licence.

the host materials for blue phosphorescent devices (Fig. 6). All these hosts show good thermal stability and excellent solution-processibility. Their frontier molecular orbitals and charge transport abilities were tuned by adjusting the numbers or connection modes of the carbazoles to facilitate efficient injection of carriers, while their singlet and triplet energy levels remain high, all above 3.44 eV and 2.87 eV, respectively. These results indicated that a tetraphenylsilane core can interrupt the conjugation effectively. Furthermore, the steric hindrance of the non-planar silicon moiety and the 3(6),9′-linked oligocarbazoles prevent the inter-molecular interactions in the solid state and thus enable formation of smooth and stable amorphous films, which allow their use as solution-processable materials.

In addition, DPSiCBP was recently reported as a host for the thermally activated delayed fluorescence (TADF) dopant 2,4,5,6-tetra(3,6-di-*tert*-butylcarbazol-9-yl)-1,3-dicyanobenzene (t4CzIPN) because of good overlap of the solid state photoluminescence (PL) emission between DPSiCBP and t4CzIPN for energy transfer, the high triplet energy of DPSiCBP (3.00 eV)[94] and good compatibility with t4CzIPN.[95] A high quantum efficiency of 18.3% was obtained in a solution-processed TADF device dispersing t4CzIPN in DPSiCBP as the emitting layer; the quantum efficiency of the device was comparable to that of vacuum evaporated TADF devices.

In the past few years, tremendous efforts have been devoted to developing bipolar hosts[96] for blue PhOLEDs to balance hole and electron injection and transportation, thus leading to a wide recombination zone. To achieve high triplet hosts, electron donating carbazole and electron withdrawing diphenylphosphine oxide units were both incorporated into the tetraphenylsilane scaffold, for example 4-diphenylphosphine oxide-4′-9*H*-carbazol-9-yl-tetraphenylsilane (CSPO)[66] (Fig. 7).

CSPO is an effective host for FCNIrpic based deep blue PhOLEDs [FCNIrpic is bis((3,5-difluoro-4-cyanophenyl)pyridine) iridium picolinate] achieving a high EQE of 22.0% with CIE (0.14, 0.18). In addition, by increasing the ratios and varying the linking modes of the carbazole units, a series of bipolar derivatives, pDCSPO, DCSPO, pTCSPO and TCSPO, were designed (Fig. 7).[73] DCSPO shows the best performance in FIrpic-doped devices for this series of compounds. By utilizing DCzSi and DPOSi as hole- and electron-transporting layers, a very high EQE of 27.5% and $\eta_{c,max}$ of 49.4 cd $A^{-1}$ are achieved in the DCSPO/FIrpic doped device. Even at 10 000 cd $m^{-2}$, the efficiencies still remain 23.0% and 41.2 cd $A^{-1}$, respectively, as shown in Fig. 8.

Compared to these single-tetraphenylsilane bridged compounds, bis-tetraphenylsilane analogues improve the solution processability and morphological stability without sacrificing the high singlet and triplet energy levels through extending the molecular size. The structures of CS2PO and DCS2PO developed for blue PhOLEDs are shown in Fig. 9.[76] DCS2PO/FIrpic doped devices fabricated by spin-coating methods show the best EL performance with $\eta_{c,max}$ 26.5 cd $A^{-1}$, $\eta_{p,max}$ 8.66 lm $W^{-1}$, and $EQE_{max}$ of 13.6%.

Moreover, a series of bis-tetraphenylsilicon bridged host materials with oxadiazole and arylamine/3,6-di-*tert*-butyl-9*H*-carbazole units as acceptor and donor groups, respectively,

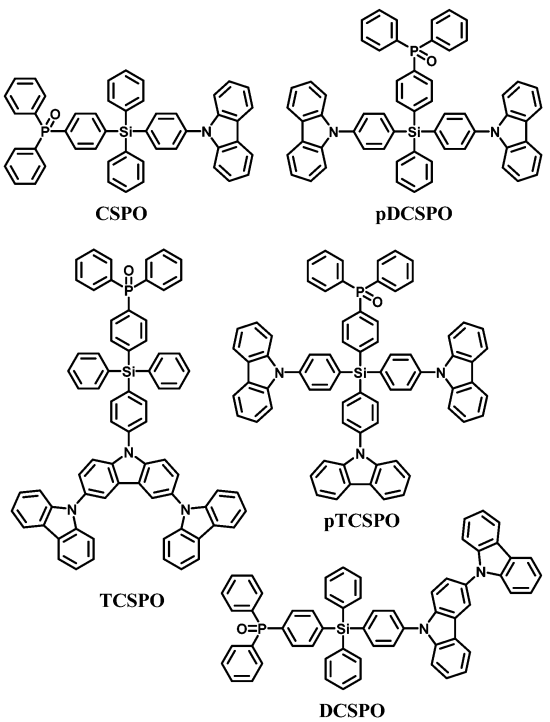


Fig. 7 Chemical structures of bipolar tetraphenylsilane hosts functionalized with carbazole and diphenylphosphine oxide.

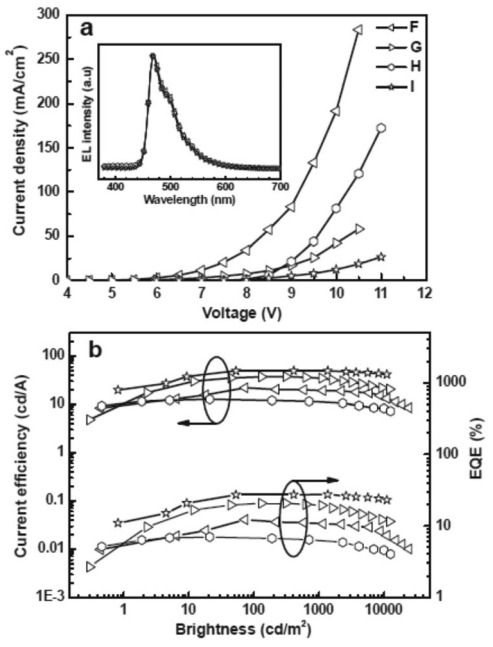


Fig. 8 (a) *J*–*V* curves for devices F–I. Inset: EL spectra of devices F–I at 8 V. (b) Curves of current efficiency and EQE *versus* brightness for devices F–I. The device configurations are: ITO/PEDOT:PSS/HTL(40 nm)/DCSPO:-FIrpic (30 nm, 8 wt%)/ETL (30 nm)/LiF (0.8 nm)/Al (100 nm), device F: HTL is NPB/mCP and ETL is TPBi; device G: HTL is NPB/mCP and ETL is DPOSi; device H: HTL is DCzSi and ETL is TPBi; device I: HTL is DCzSi and ETL is DPOSi. Reproduced with permission from ref. 73, Copyright 2012 Wiley-VCH Verlag GmbH & Co. KGaA, Weinheim.


This journal is © The Royal Society of Chemistry 2015

Open Access Article. Published on 14 augustus 2015. Downloaded on 8/10/2025 15:53:28.
This article is licensed under a Creative Commons Attribution 3.0 Unported Licence.

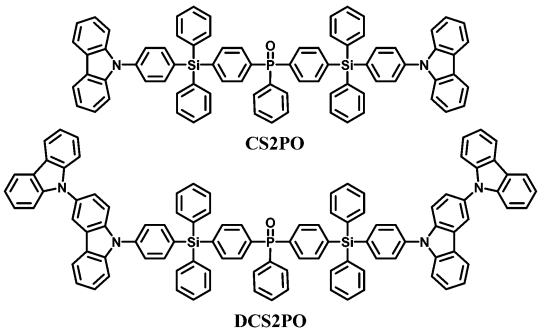


Fig. 9 Chemical structures of bipolar bis-tetraphenylsilicon bridged hosts functionalized with carbazole and phenylphosphine oxide.

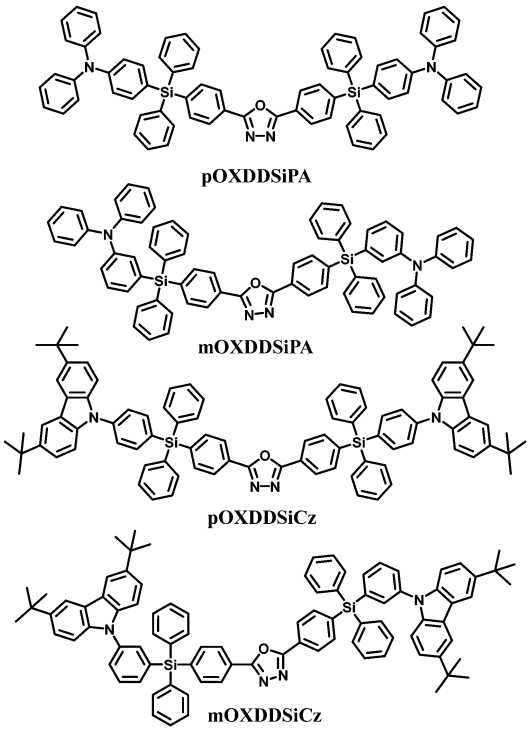


Fig. 10 Chemical structures of bipolar bis-tetraphenylsilicon bridged hosts functionalized with oxadiazole and arylamine/carbazole.

are also used for blue PhOLEDs: namely pOXDDSiPA, mOXDDSiPA, pOXDDSiCz, and mOXDDSiCz (Fig. 10).[69] These compounds exhibit similar energy levels and higher glass transition temperatures (92–190 °C) relative to the single-silicon-bridged congeners. The combination of the tetra-*meta*-position linking topology and the diphenylamine group imparts mOXDDSiPA with both a relatively high triplet energy (2.72 eV) and a high-lying HOMO level (−5.30 eV). As a result, the best EL performance was achieved for the mOXDDSiPA–FIrpic blue device, with $\eta_{c,max}$ of 23.4 cd $A^{-1}$, $\eta_{p,max}$ of 10.2 lm $W^{-1}$ and $EQE_{max}$ of 10.7%. Moreover, the current efficiency remains as high as 23.3 cd $A^{-1}$ at the luminance of 100 cd $m^{-2}$, and even at the high luminance of 1000 cd $m^{-2}$, the efficiency is 17.7 cd $A^{-1}$.

Arylsilane derivatives can also be used as hole and exciton blocking materials due to their deep HOMO levels. Kim *et al.*[53]

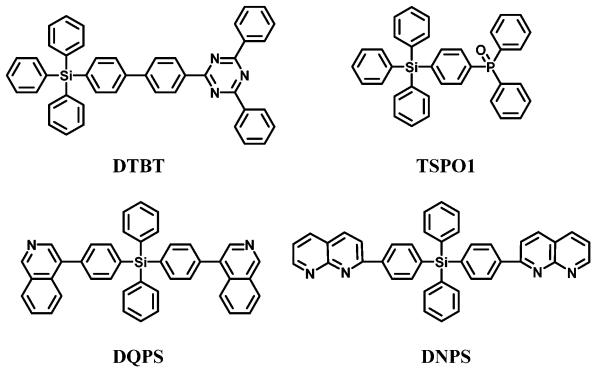


Fig. 11 Chemical structures of electron-transporting and hole/exciton blocking materials.

reported a new triazine functionalized tetraphenylsilane compound, 2,4-diphenyl-6-(4′-triphenylsilanyl-biphenyl-4-yl)-1,3,5-triazine (DTBT) (Fig. 11). The triazine moiety provides high electron mobility associated with a deep HOMO level and the tetraphenylsilane moiety endows high thermal and chemical stability and amorphous properties. Green electrophosphorescent devices fabricated using DTBT as the hole-blocking layer and *N*,*N*′-dicarbazolyl-4,4′-biphenyl (CBP) doped with *fac*-tris-(2-phenylpyridine)iridium [$Ir(ppy)_3$] as the emitting layer showed $EQE_{max}$ of 17.5% with $\eta_{p,max}$ of 47.8 lm $W^{-1}$. However, the low triplet energy of 2.44 eV limited the use of DTBT in blue PhOLEDs.

Diphenylphosphine oxide derivatives are suitable as electron-transport-type high-triplet-energy exciton blocking materials. Therefore, Lee *et al.*[67] introduced diphenylphosphine oxide-4-(triphenylsilyl)phenyl (TSPO1) (Fig. 11) which showed a sufficiently high triplet energy of 3.36 eV to block excitons and to suppress the triplet exciton quenching of the deep blue phosphor FCNIrpic. In addition, the LUMO of the TSPO1 (−2.52 eV) is lowered for efficient electron injection, owing to the diphenylphosphine oxide substituent. Meanwhile, the HOMO of TSPO1 (−6.79 eV) is suitable for hole blocking.

Recently, tetraphenylsilane derivatives with a wide energy gap (≈3.5 eV) containing quinoline (DQPS) and naphthyridine (DNPS) electron-withdrawing groups have been used as electron transporting materials (Fig. 11).[79]

The different electron transporting and hole/exciton blocking properties of the silane derivatives were investigated in multilayered device structures. The $E_T$ values are 2.27 eV and 2.54 eV for DQPS and DNPS, respectively. Using *fac*-$Ir(ppy)_3$ as the emitter, EQE of 15.4% corresponding to $\eta_{c,max}$ 56.2 cd $A^{-1}$ was obtained with a maximum power efficiency $\eta_{p,max}$ 58.9 lm $W^{-1}$ with DNPS as the electron transporting material, combined with 2,9-dimethyl-4,7-diphenyl-1,10-phenanthroline (DMP) as the hole blocking layer: this is higher efficiency than for a conventional $Alq_3$ device. Changing from DNPS to DQPS lowered the efficiency to 11.4% EQE, with 41.4 cd $A^{-1}$ and 32.5 lm $W^{-1}$. These data indicate that the electron transporting ability is higher for DNPS (naphthyridine groups) than for DQPS (quinoline groups).

Open Access Article. Published on 14 augustus 2015. Downloaded on 8/10/2025 15:53:28.
This article is licensed under a Creative Commons Attribution 3.0 Unported Licence.

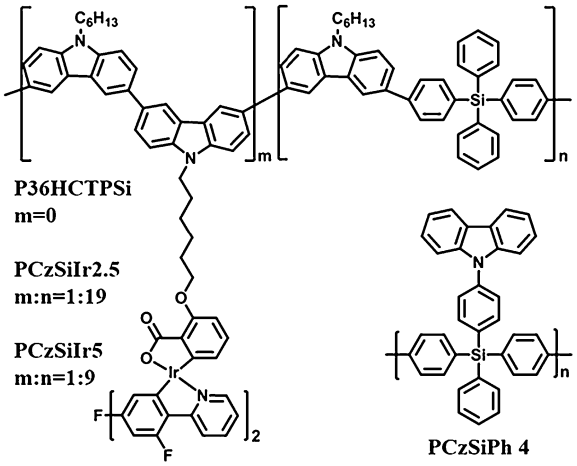


Fig. 12 Chemical structures of polymers incorporating tetraphenylsilane fragments.

In addition to being an effective core structure for small molecule optoelectronic materials, tetraphenylsilane has also been inserted into the backbone of polycarbazole to confine the conjugation length. Ma *et al.*[60] synthesized a copolymer (P36HCTPSi) (Fig. 12) based on *N*-hexyl-3,6-carbazole and tetraphenylsilane with a wide band gap (3.26 eV) (Table 1).

Table 1 Physical properties of arylsilane-based small molecules

| Material | HOMO [eV] | LUMO [eV] | $E_T$ [eV] | $T_g$ [°C] | $T_d$ [°C] | Ref. |
|---|---|---|---|---|---|---|
| $Si(PhTPAOXD)_4$ | −5.52 | −2.42 | — | 174 | 461 | 44 |
| $PhSi(PhTPAOXD)_3$ | −5.50 | −2.45 | — | 163 | 464 | 44 |
| $Ph_2Si(PhTPAOXD)_2$ | −5.54 | −2.29 | — | 120 | 467 | 44 |
| $Ph_3Si(PhTPAOXD)$ | −5.56 | −2.41 | — | 83 | 462 | 44 |
| $Ph_2Si(Ph(NPA)_2)_2$ | −5.2 | −2.1 | — | 95 | — | 45 |
| UGH1 | −7.2[a] | −2.6[b] | 3.16 | 26 | — | 46 |
| UGH2 | −7.2[a] | −2.8[b] | 3.18 | — | — | 46 |
| UGH3 | −7.2[a] | −2.8[b] | 3.1 | 46 | — | 47 |
| UGH4 | −7.2[a] | −2.8[b] | 3.1 | 53 | — | 47 |
| BSB | −6.49 | −2.33 | 2.76 | 100 | — | 57 |
| BST | −6.25 | −2.47 | 2.58 | 113 | — | 57 |
| CzSi | −6.0[a] | −2.5[b] | 3.02 | 131 | 392 | 52 |
| DMSiCBP | −5.58 | −1.92 | 3.03 | 90 | — | 61 |
| DPSiCBP | −5.58 | −1.95 | 3.02 | 120 | 459 | 61 |
| DCzSiCz | −5.41 | −2.01 | 2.97 | 162 | 501 | 70 |
| DDCzSi | −5.42 | −2.01 | 2.95 | — | 512 | 70 |
| DTCzSi | −5.44 | −2.12 | 2.87 | — | 571 | 70 |
| CSPO | −6.03 | −2.49 | 3.01 | 107 | 420 | 66 |
| pDCSPO | −5.59 | −2.20 | 3.02 | 124 | 433 | 73 |
| DCSPO | −5.43 | −2.19 | 2.97 | 140 | 420 | 73 |
| pTCSPO | −5.57 | −2.20 | 3.02 | 173 | 529 | 73 |
| TCSPO | −5.46 | −2.20 | 2.89 | 184 | 512 | 73 |
| CS2PO | −5.56 | −2.21 | 3.04 | 159 | 485 | 76 |
| DCS2PO | −5.43 | −2.19 | 2.97 | 199 | 521 | 76 |
| pOXDDSiPA | −5.31 | −2.29 | 2.67 | 123 | 469 | 69 |
| mOXDDSiPA | −5.30 | −2.27 | 2.72 | 92 | 456 | 69 |
| pOXDDSiCz | −5.49 | −2.31 | 2.67 | 190 | 435 | 69 |
| mOXDDSiCz | −5.46 | −2.28 | 2.73 | 158 | 460 | 69 |
| DTBT | −6.5[a] | −3.0 | 2.44 | — | — | 53 |
| TSPO1 | −6.79 | −2.52 | 3.36 | — | — | 67 |
| DQPS | −6.01[a] | −3.58[b] | 2.27 | 81 | 535 | 79 |
| DNPS | −6.05[a] | −3.44[b] | 2.54 | 115 | 532 | 79 |

[a] Measured by UPS. [b] Calculated by HOMO and bandgap.

Green and blue phosphorescent PLEDs were obtained by using P36HCTPSi as a host for iridium complexes: green $Ir(mppy)_3$ 27.6 cd $A^{-1}$; $L_{max}$ 10 000 cd $m^{-2}$, and blue FIrpic 3.4 cd $A^{-1}$; $L_{max}$ 1500 cd $m^{-2}$, respectively. Carbazole-*alt*-tetraphenylsilane copolymers PCzSiIr2.5 and PCzSiIr5 grafted with various content of covalently bonded FIrpic were also studied (Fig. 12).[64] The mainly blue emission from FIrpic indicated efficient energy transfer from the polymer backbone to the iridium guest. The greatest advantage of this covalent host–guest strategy is to suppress the potential host–guest phase separation. The luminance efficiency of these blue polymer devices reached 2.3 cd $A^{-1}$.

Recently, our group reported a hybrid polymeric host (PCzSiPh)[77] with carbazole as pendants on a polytetraphenylsilane main chain (Fig. 12). PCzSiPh has a wide bandgap and high triplet energy. Meanwhile, the polymer also exhibits good solubility in standard organic solvents, combined with high thermal and morphological stability. Notably, PCzSiPh/FIrpic devices, with a solution-processed emitter layer, exhibit $EQE_{max}$ of 14.3% (29.3 cd $A^{-1}$, 10.4 lm $W^{-1}$; CIE 0.149, 0.322) which are comparable to state-of-the-art literature data using polymer hosts for a blue dopant emitter. The versatility of PCzSiPh extends to deep blue PhOLEDs based on FIr6 and FCNIrpic with high efficiencies of 11.3 cd $A^{-1}$ (CIE 0.176, 0.272) and 8.6 cd $A^{-1}$ (0.143, 0.181), respectively, as shown in Fig. 13.[77]

### 2.3 Polyhedral oligomeric silsesquioxanes (POSS)-based optoelectronic materials

Polyhedral oligomeric silsesquioxanes (POSS) are cube-shaped nanoparticles in which the conformationally rigid $T_8$ unit can be functionalized with eight organic groups. This hybridization leads to useful properties, including high thermal stability in

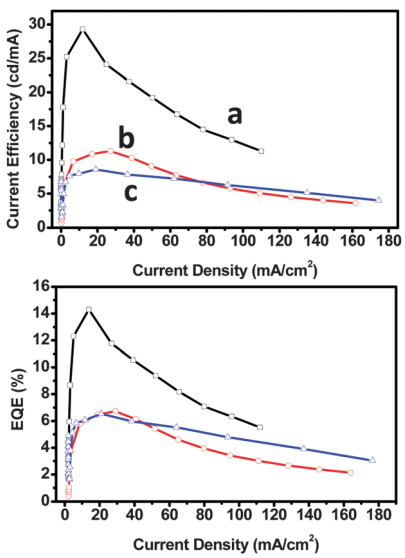


Fig. 13 Current efficiency–current density characteristics (top panel) and external quantum efficiency–current density characteristics (bottom panel) for devices a–c. The device configurations are: ITO/PEDOT:PSS/PCzSiPh:dopant (50 nm)/Tm3PyPB (5 nm)/TPBi (30 nm)/LiF/Al, dopant is 10% FIrpic, 10% FIr6 and 3% FCNIrpic for devices a, b and c, respectively.


This journal is © The Royal Society of Chemistry 2015

Open Access Article. Published on 14 augustus 2015. Downloaded on 8/10/2025 15:53:28.
This article is licensed under a Creative Commons Attribution 3.0 Unported Licence.

air, good solubility in common solvents and adhesion to a number of substrates.[97,98] In the context of electroluminescent devices, POSS macromolecules bearing carrier-transporting moieties or chromophores combine the advantages of both small-molecule and polymer light-emitting materials, *e.g.*, high purity and solution processability. In general, POSS-containing polymer LEDs exhibit improved external quantum efficiency, luminance, and color stability due to the diminished interchain interactions.

Heeger's group[18] first introduced POSS units as end groups to poly(2-methoxy-5-(2-ethylhexyloxy)-1,4-phenylenevinylene) (MEH-PPV) (MEH-PPV–POSS), and to poly(9,9-dihexylfluorenyl-2,7-diyl) (PHF) (PHF–POSS) (Fig. 14). Compared with the corresponding polymers MEH-PPV and PHF, MEH-PPV–POSS and PHF–POSS have improved thermal stability and decreased excimer formation by chemically incorporating bulky POSS into the conjugated polymer chain. Meanwhile they have identical photophysical properties. Devices made from POSS end-capped polymers exhibit higher brightness and higher external quantum efficiency ($L_{max}$ 1320 cd m$^{-2}$ at 3.5 V and $\eta_{ext}$ = 2.2% for MEH-PPV–POSS) compared to that of MEH-PPV (230 cd m$^{-2}$ at 3.5 V and $\eta_{ext}$ 1.5%).

Shim's group[19] subsequently reported copolymers PF–POSS (Fig. 15) where POSS units are appended to the polyfluorene backbone using an alkoxy spacer. PL spectra of the copolymers are identical to that of polyfluorene, showing blue emission and no signs of aggregation or excimer formation. On the other hand, the fluorescence quantum yields ($\Phi_{FL}$) of the copolymers were higher than that of poly(9,9-dialkylfluorene) in solution and in the solid state. Because the POSS unit reduces the fluorescence quenching, $\Phi_{FL}$ of PF–POSS derivatives are enhanced as the POSS ratio increases. Electroluminescence spectra of the copolymers revealed a blue shift in emission as the silsesquioxane content of the copolymers was increased. Blue OLEDs based on PF–POSS showed a low turn-on voltage of 3.7–4.4 V, a brightness of 350–1010 cd m$^{-2}$, and EQEs of 0.11–0.36%.

Another successful approach to hybrid organic–inorganic polymers is to attach peripheral polymers to a POSS core. Lin *et al.*[20] prepared a starlike polyfluorene derivative, PFO-SQ using a variant of the octabromosilsesquioxane core where an ethylene bridge is inserted between the silicon vertices and phenyl groups (Fig. 16). Pre-synthesized bromide-terminated polyfluorene was coupled to the octa(2-(4-bromophenyl)ethyl)-octasilsesquioxane core *via* Yamamoto coupling. (The bromine end-groups were not replaced by end-capping). A comparison of PFO-SQ with linear PFO shows that interchain packing is significantly disrupted and chain mobility is reduced in the PFO-SQ due to its branched architecture. Whereas PFO shows distinct glass (63 °C), cold crystallization (93 °C) and melting (154 °C) transitions, the PFO-SQ displayed only a small melting peak at 158 °C. The reduced interchain packing leads to enhancement in the colour stability of PFO-SQ as the green emission band, attributed to aggregation/excimer formation and/or fluorenone defects, is significantly suppressed. The solid state photoluminescence quantum yield (PLQY) of PFO-SQ ($\Phi_{FL}$ = 64%) is also slightly improved over its linear analogue ($\Phi_{FL}$ = 55%) due to reduced aggregation quenching. A single-active-layer device using PFO-SQ demonstrated a brightness of 5430 cd m$^{-2}$ and a current density of 0.844 A cm$^{-2}$ at 8.8 V, with the maximum luminescence intensity and EQE of the device almost twice that of a comparable PFO device.

Small molecule chromophores have also been attached to the POSS core. Sellinger *et al.*[26] fabricated two hybrid materials with varying extent of pyrene-functionalized peripheries (Fig. 17). In contrast to most pyrene derivatives that are highly crystalline and non-emissive in the solid state, these compounds are completely amorphous and exhibit very strong photoluminescence in thin films. Furthermore, they offer many advantages

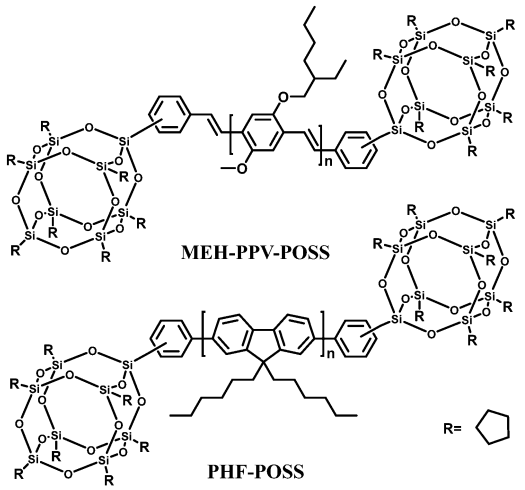


Fig. 14 Chemical structures of MEH-PPV–POSS and PHF–POSS.

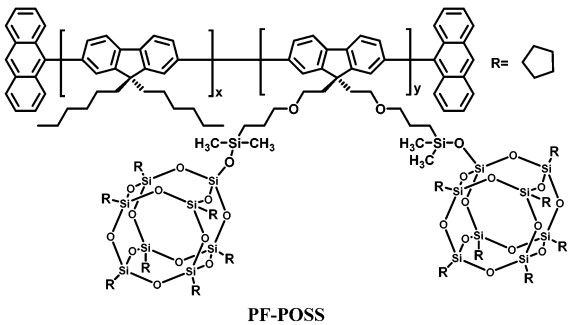


Fig. 15 Chemical structure of PF–POSS.

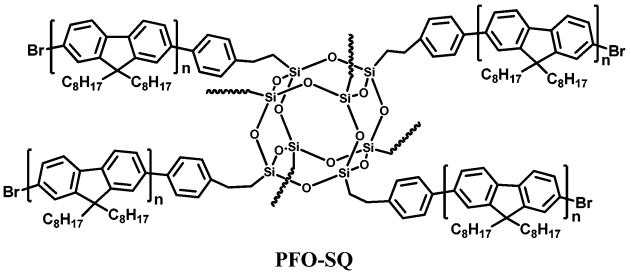


Fig. 16 Chemical structure of PFO-SQ.

Open Access Article. Published on 14 augustus 2015. Downloaded on 8/10/2025 15:53:28.
This article is licensed under a Creative Commons Attribution 3.0 Unported Licence.

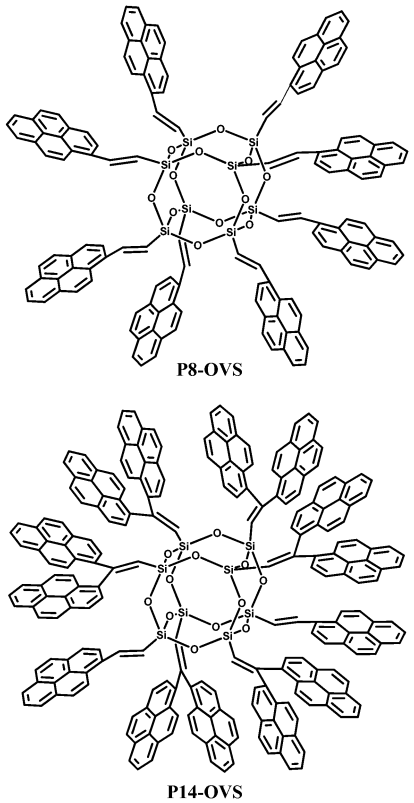


Fig. 17 Chemical structures of P8-OVS and P14-OVS.

for OLEDs including ease of synthesis, high-glass-transition temperatures ($T_g$), good film-forming properties, low polydispersity, and high-purity *via* column chromatography. Preliminary unoptimized OLED external quantum and current efficiencies of 2.63% and 8.28 cd $A^{-1}$, respectively, were reported.

To improve the performance of OLEDs, Jabbour *et al.*[30] developed iridium-complex anchored POSS macromolecules (Fig. 18). Simultaneous attachment of the host materials and Ir-complex moieties to the POSS core should reduce host–guest phase separation. Furthermore, incorporation of the sterically bulky groups is helpful for decreasing the interaction among the iridium complexes. Monochromatic OLEDs based on these phosphorescent POSS materials show $EQE_{max}$ values of 5–9%, which can be driven at less than 10 V for a luminance of 1000 cd $m^{-2}$.

The white-emitting devices with red, green and blue (R, G, and B)-POSS emitters show $EQE_{max}$ of 8%, $\eta_{pmax}$ 8.1 lm $W^{-1}$, and CIE (0.36, 0.39) at $L$ 1000 cd $m^{-2}$. Encouraging efficiency values are achieved for the devices based on POSS derivatives dual-functionalized with hole-transporting and Ir-complex moieties without using host materials. This work demonstrates that attachment of both triplet-dye and carrier-transporting moieties is a viable approach to solution-processable electrophosphorescent devices.

In a conceptually similar strategy, the combination of carbazole and platinum-complex moieties on the same POSS core effectively dilutes the concentration of the complex in a single molecule,[33] thereby adjusting the monomer and excimer/aggregate emission (Fig. 19). OLEDs using these POSS macromolecules exhibit significantly higher efficiencies when compared to devices based on a physical blend of the platinum complexes and the polymer matrix. Furthermore, the ratio of monomer/excimer emission intensity in the EL spectrum and the device efficiency both increase with decreased platinum-complex content within the POSS macromolecules.

### 2.4 Polysiloxane-based host materials for blue PhOLEDs

Recently, the synthesis and unique optoelectronic properties of polysiloxane derivatives as hosts for blue PhOLEDs have been exploited by our group. Various high triplet energy moieties have been introduced into the polysiloxane main-chain while

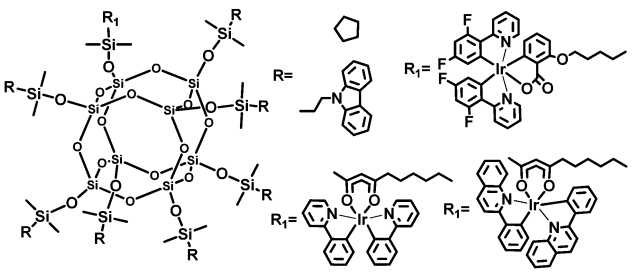

Fig. 18 Chemical structures of iridium-complex anchored polyhedral oligomeric silsesquioxane (POSS) macromolecules.

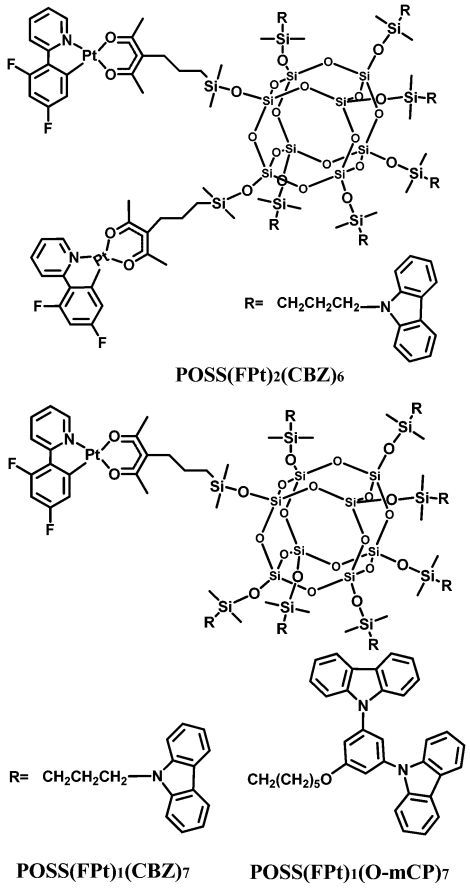


Fig. 19 Chemical structures of platinum-complex anchored polyhedral oligomeric silsesquioxane (POSS) macromolecules.


This journal is © The Royal Society of Chemistry 2015

Open Access Article. Published on 14 augustus 2015. Downloaded on 8/10/2025 15:53:28.
This article is licensed under a Creative Commons Attribution 3.0 Unported Licence.

maintaining their intrinsic energy levels and charge transporting abilities. Compared to a single functional unit, the thermal and morphological stability is significantly improved. Meanwhile, the polysiloxane hybrids show excellent solubility, film-forming abilities and miscibility to guest iridium complexes. In addition to the merits of arylsilanes or polyhedral oligomeric silsesquioxanes, the intrinsic polymer structures are applicable for solution processing techniques, such as spin-coating and ink-jet printing, which are more suitable than thermal evaporation for large-area devices. Moreover, polysiloxanes present a higher transparency than POSS-based materials. Therefore, polysiloxanes are excellent candidates for solution-processed blue PhOLEDs.

A ladder polysilsesquioxane containing 3-methyl-1,5-diphenylbenzene substituents (Tp-LPSQ) was the first polysiloxane host material for solution-processed blue PhOLEDs (Fig. 20).[34] Polymer Tp-LPSQ was obtained by a supramolecular template directed coupling polymerization. The ladder polysilsesquioxane possesses excellent resistance to thermal, chemical and irradiation degradation due to the stable double-stranded molecular structure. Tp-LPSQ also exhibits a wide bandgap of *ca.* 4.0 eV and high $E_T$ of 2.82 eV. The FIrpic-based OLED with a traditional device configuration reaches a brightness of $L_{max}$ 883 cd $m^{-2}$, $\eta_{c,max}$ 8.7 cd $A^{-1}$, and $\eta_{p,max}$ 3.1 lm $W^{-1}$ with EQE of 4.6%.

A FIrpic-based OLED was also fabricated with a cyclic polysiloxane host and dibenzothiophene side groups (BS-PSQ) (Fig. 21).[35] The molecule has similar thermal and optical properties to the POSS-based materials, in addition to a wide band gap of *ca.* 3.88 eV and a high $E_T$ of 2.84 eV. The device exhibited $\eta_{c,max}$ 4.5 cd $A^{-1}$ (2.4 lm $W^{-1}$, EQE 2.5%). However, the PL spectra of BS-PSQ indicated aggregation in the solid film. To solve this problem, a ladder polysilsesquioxane (BS-LPSQ) based on the same pendant was developed (Fig. 21).[36] The limited conformational freedom of the ladder analogue is expected to reduce the electron delocalization of the conjugated polymer and thus suppress aggregation. Thus, a slightly enhanced performance was realized with $\eta_{c,max}$ 5.9 cd $A^{-1}$ (3.1 lm $W^{-1}$, EQE 2.9%).

The use of linear polysiloxane instead of ladder or cyclic systems is advantageous in that the desired product can be more easily synthesized and the properties can be manipulated more freely by expanding the range of functional units. In addition, the alkyl chain bridge between the silicon atom and functional pendants can be eliminated, thus avoiding aggregation due to reduced mobility of pendants.

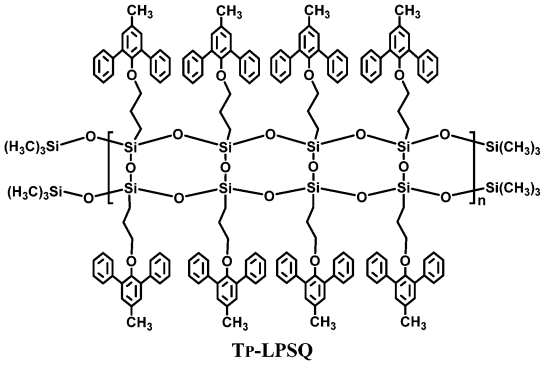


Fig. 20 Chemical structure of Tp-LPSQ.

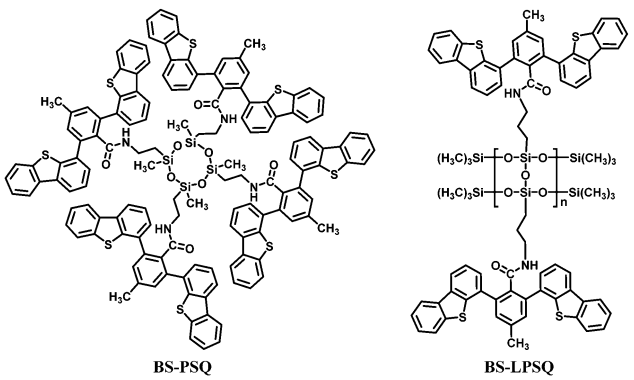


Fig. 21 Chemical structures of BS-PSQ and BS-LPSQ.

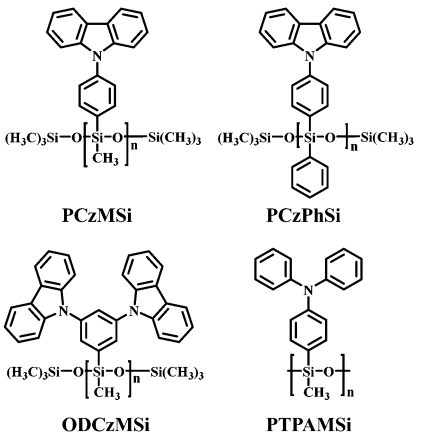


Fig. 22 Chemical structures of hole-transporting linear polysiloxane hosts.

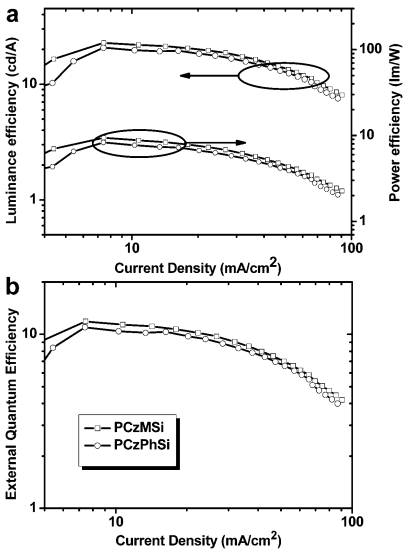


Fig. 23 (a) Luminance efficiency and power efficiency *versus* current density of PCzMSi and PCzPhSi. (b) External quantum efficiency *versus* current density of PCzMSi and PCzPhSi.

Open Access Article. Published on 14 augustus 2015. Downloaded on 8/10/2025 15:53:28.
This article is licensed under a Creative Commons Attribution 3.0 Unported Licence.

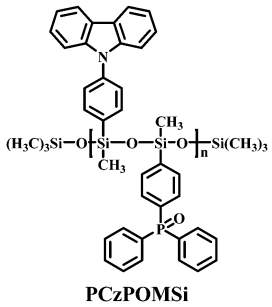


Fig. 24 Chemical structure of PCzPOMSi.

Therefore, a wide array of linear polysiloxane-based hole-dominant hosts were synthesized by attaching popular high triplet energy carbazole or arylamine units (Fig. 22).[39–41] The flexible polysiloxane main chain with methyl or phenyl groups attached to Si enhances the formation of morphologically stable amorphous films and improves the solubility. The FIrpic-based OLEDs using these polysiloxane hosts show good overall performance with maximum EQE of >10% at practical luminance, which are among the most efficient solution-processed blue PhOLEDs, suggesting the superiority of linear polysiloxane hosts. Typically, using PCzMSi or PCzPhSi as the blue phosphorescent host, relatively low turn-on voltages of 5.5 and 5.1 V, $EQE_{max}$ 11.9% and 11.0%, $\eta_{c,max}$ 22.8 and 20.7 cd $A^{-1}$ are obtained, respectively, as shown in Fig. 23.[39]

Based on condensation polymerization reactions, a bipolar polysiloxane host has been synthesized. This design strategy serves to balance the hole and electron transport within the emitting layer. PCzPOMSi (Fig. 24) has been used to host the deep blue emitter FCNIrpic.[38] A PCzPOMSi/FCNIrpic-based device shows a turn-on voltage of 7.7 V, $EQE_{max}$ 4% and $\eta_{c,max}$ of 8.5 cd $A^{-1}$. Therefore, polysiloxane derivatives are well established as host materials for solution-processed PhOLEDs.

## 3. Conclusions and perspectives

In this review, we have demonstrated that arylsilanes and siloxanes are very promising optoelectronic materials with particular importance in OLED applications. The key features of these materials are their structural versatility, good solubility and excellent resistance to thermal, chemical and irradiation degradations. However, it is clear that considerable critical challenges still remain to be solved. We expect that future research will emphasize the following areas of development, which should favour the realization of higher efficiency and longer-lifetime OLEDs based on arylsilanes and siloxanes:

(1) In comparison to small molecules, polymers have the advantage of being applicable in larger area display and lighting technologies at much lower manufacturing costs *via* solution processing deposition techniques because of their good film-forming ability. Thus, new polymers based on arylsilanes and siloxanes are in demand.

(2) Phosphorescent OLEDs using polysiloxanes or polyarylsilanes as hosts for iridium complexes, or bearing the complexes as pendant units, offer scope for further enhancement of device efficiency, for both monochromatic and white-emitting devices. New organometallic phosphors and TADF molecules, especially deep blue emitters, should be explored with these hosts.

(3) Most of the reported arylsilanes and siloxanes possess good hole-transporting ability. Therefore, the solution processable electron transporting analogues based on small molecules or polymers with high thermal stability, high electron mobility and high triplet energy are critical for extending their applications in OLEDs.

## Acknowledgements

The financial supports of NSFC (No. 21104002 & 51221002) and Beijing Higher Education Young Elite Teacher Project (YETP0491) are gratefully acknowledged. The work in Durham was funded by EPSRC.

## Notes and references

1 C. W. Tang and S. VanSlyke, *Appl. Phys. Lett.*, 1987, **51**, 913–915.
2 R. Holmes, S. Forrest, Y. J. Tung, R. Kwong, J. Brown, S. Garon and M. Thompson, *Appl. Phys. Lett.*, 2003, **82**, 2422–2424.
3 S. Tokito, T. Iijima, Y. Suzuri, H. Kita, T. Tsuzuki and F. Sato, *Appl. Phys. Lett.*, 2003, **83**, 569–571.
4 J. Kavitha, S. Y. Chang, Y. Chi, J. K. Yu, Y. H. Hu, P. T. Chou, S. M. Peng, G. H. Lee, Y. T. Tao and C. H. Chien, *Adv. Funct. Mater.*, 2005, **15**, 223–229.
5 Y. Sakamoto, T. Suzuki, A. Miura, H. Fujikawa, S. Tokito and Y. Taga, *J. Am. Chem. Soc.*, 2000, **122**, 1832–1833.
6 M. Ikai, S. Tokito, Y. Sakamoto, T. Suzuki and Y. Taga, *Appl. Phys. Lett.*, 2001, **79**, 156–158.
7 A. P. Kulkarni, C. J. Tonzola, A. Babel and S. A. Jenekhe, *Chem. Mater.*, 2004, **16**, 4556–4573.
8 N. Satoh, J. S. Cho, M. Higuchi and K. Yamamoto, *J. Am. Chem. Soc.*, 2003, **125**, 8104–8105.
9 G. Hughes and M. R. Bryce, *J. Mater. Chem.*, 2005, **15**, 94–107.
10 Y. Shirota and H. Kageyama, *Chem. Rev.*, 2007, **107**, 953–1010.
11 H. Sasabe, E. Gonmori, T. Chiba, Y. J. Li, D. Tanaka, S. J. Su, T. Takeda, Y. J. Pu, K. i. Nakayama and J. Kido, *Chem. Mater.*, 2008, **20**, 5951–5953.
12 S. J. Su, T. Chiba, T. Takeda and J. Kido, *Adv. Mater.*, 2008, **20**, 2125–2130.
13 S. J. Su, Y. Takahashi, T. Chiba, T. Takeda and J. Kido, *Adv. Funct. Mater.*, 2009, **19**, 1260–1267.
14 L. Xiao, S. J. Su, Y. Agata, H. Lan and J. Kido, *Adv. Mater.*, 2009, **21**, 1271–1274.
15 S. J. Su, H. Sasabe, Y. J. Pu, K. i. Nakayama and J. Kido, *Adv. Mater.*, 2010, **22**, 3311–3316.

 This journal is © The Royal Society of Chemistry 2015

Open Access Article. Published on 14 augustus 2015. Downloaded on 8/10/2025 15:53:28.
This article is licensed under a Creative Commons Attribution 3.0 Unported Licence.

16 H. Ye, D. Chen, M. Liu, S. J. Su, Y. F. Wang, C. C. Lo, A. Lien and J. Kido, *Adv. Funct. Mater.*, 2014, **24**, 3268–3275.
17 B. A. Kamino and T. P. Bender, *Chem. Soc. Rev.*, 2013, **42**, 5119–5130.
18 S. Xiao, M. Nguyen, X. Gong, Y. Cao, H. Wu, D. Moses and A. Heeger, *Adv. Funct. Mater.*, 2003, **13**, 25–29.
19 J. Lee, H. J. Cho, B.-J. Jung, N. S. Cho and H. K. Shim, *Macromolecules*, 2004, **37**, 8523–8529.
20 W. J. Lin, W. C. Chen, W. C. Wu, Y. H. Niu and A. K. Y. Jen, *Macromolecules*, 2004, **37**, 2335–2341.
21 I. Imae and Y. Kawakami, *J. Mater. Chem.*, 2005, **15**, 4581–4583.
22 A. Sellinger, R. Tamaki, R. M. Laine, K. Ueno, H. Tanabe, E. Williams and G. E. Jabbour, *Chem. Commun.*, 2005, 3700–3702.
23 H. Cho, D. H. Hwang, J. I. Lee, Y. K. Jung, J. H. Park, J. Lee, S. K. Lee and H. K. Shim, *Chem. Mater.*, 2006, **18**, 3780–3787.
24 K. B. Chen, Y. P. Chang, S. H. Yang and C. S. Hsu, *Thin Solid Films*, 2006, **514**, 103–109.
25 J. D. Froehlich, R. Young, T. Nakamura, Y. Ohmori, S. Li, A. Mochizuki, M. Lauters and G. E. Jabbour, *Chem. Mater.*, 2007, **19**, 4991–4997.
26 M. Y. Lo, C. Zhen, M. Lauters, G. E. Jabbour and A. Sellinger, *J. Am. Chem. Soc.*, 2007, **129**, 5808–5809.
27 Q. Zhou, J. Zhang, Z. Ren, S. Yan, P. Xie and R. Zhang, *Macromol. Rapid Commun.*, 2008, **29**, 1259–1263.
28 K. L. Chan, P. Sonar and A. Sellinger, *J. Mater. Chem.*, 2009, **19**, 9103–9120.
29 M. Singh, H. S. Chae, J. D. Froehlich, T. Kondou, S. Li, A. Mochizuki and G. E. Jabbour, *Soft Matter*, 2009, **5**, 3002–3005.
30 X. Yang, J. D. Froehlich, H. Chae, S. Li, A. Mochizuki and G. E. Jabbour, *Adv. Funct. Mater.*, 2009, **19**, 2623–2629.
31 V. Ervithayasuporn, J. Abe, X. Wang, T. Matsushima, H. Murata and Y. Kawakami, *Tetrahedron*, 2010, **66**, 9348–9355.
32 Y. Lim, Y. S. Park, Y. Kang, D. Y. Jang, J. H. Kim, J. J. Kim, A. Sellinger and D. Y. Yoon, *J. Am. Chem. Soc.*, 2010, **133**, 1375–1382.
33 X. Yang, J. D. Froehlich, H. S. Chae, B. T. Harding, S. Li, A. Mochizuki and G. E. Jabbour, *Chem. Mater.*, 2010, **22**, 4776–4782.
34 Z. Ren, Z. Chen, W. Fu, R. Zhang, F. Shen, F. Wang, Y. Ma and S. Yan, *J. Mater. Chem.*, 2011, **21**, 11306–11311.
35 Z. Ren, R. Zhang, Y. Ma, F. Wang and S. Yan, *J. Mater. Chem.*, 2011, **21**, 7777–7781.
36 Z. Ren, D. Sun, H. Li, Q. Fu, D. Ma, J. Zhang and S. Yan, *Chem. – Eur. J.*, 2012, **18**, 4115–4123.
37 X. H. Yang, T. Giovenzana, B. Feild, G. E. Jabbour and A. Sellinger, *J. Mater. Chem.*, 2012, **22**, 12689–12694.
38 D. Sun, Q. Fu, Z. Ren, H. Li, D. Ma and S. Yan, *Polym. Chem.*, 2013, **5**, 220–226.
39 D. Sun, Q. Fu, Z. Ren, W. Li, H. Li, D. Ma and S. Yan, *J. Mater. Chem. C*, 2013, **1**, 5344–5350.
40 D. Sun, Z. Yang, Z. Ren, H. Li, M. R. Bryce, D. Ma and S. Yan, *Chem. – Eur. J.*, 2014, **20**, 16233–16241.
41 D. Sun, Z. Yang, X. Sun, H. Li, Z. Ren, J. Liu, D. Ma and S. Yan, *Polym. Chem.*, 2014, **5**, 5046–5052.
42 T. Zhang, J. Wang, M. Zhou, L. Ma, G. Yin, G. Chen and Q. Li, *Tetrahedron*, 2014, **70**, 2478–2486.
43 D. Sun, X. Zhou, J. Liu, X. Sun, H. Li, Z. Ren, D. Ma, M. R. Bryce and S. Yan, *ACS Appl. Mater. Interfaces*, 2015, DOI: 10.1021/am507592s.
44 L. H. Chan, H. C. Yeh and C. T. Chen, *Adv. Mater.*, 2001, **13**, 1637–1641.
45 L. H. Chan, R. H. Lee, C. F. Hsieh, H. C. Yeh and C. T. Chen, *J. Am. Chem. Soc.*, 2002, **124**, 6469–6479.
46 R. Holmes, B. D'Andrade, S. Forrest, X. Ren, J. Li and M. Thompson, *Appl. Phys. Lett.*, 2003, **83**, 3818–3820.
47 X. Ren, J. Li, R. J. Holmes, P. I. Djurovich, S. R. Forrest and M. E. Thompson, *Chem. Mater.*, 2004, **16**, 4743–4747.
48 J. U. Kim, H. B. Lee, J. S. Shin, Y. H. Kim, Y. K. Joe, H. Y. Oh, C. G. Park and S. K. Kwon, *Synth. Met.*, 2005, **150**, 27–32.
49 X. M. Liu, C. He, J. Huang and J. Xu, *Chem. Mater.*, 2005, **17**, 434–441.
50 X. M. Liu, J. Xu, X. Lu and C. He, *Org. Lett.*, 2005, **7**, 2829–2832.
51 R. H. Lee, H. F. Hsu, L. H. Chan and C. T. Chen, *Polymer*, 2006, **47**, 7001–7012.
52 M. H. Tsai, H. W. Lin, H. C. Su, T. H. Ke, C. C. Wu, F. C. Fang, Y. L. Liao, K. T. Wong and C. I. Wu, *Adv. Mater.*, 2006, **18**, 1216–1220.
53 J. W. Kang, D. S. Lee, H. D. Park, Y. S. Park, J. W. Kim, W. I. Jeong, K. M. Yoo, K. Go, S. H. Kim and J. J. Kim, *J. Mater. Chem.*, 2007, **17**, 3714–3719.
54 P. I. Shih, C. H. Chien, C. Y. Chuang, C. F. Shu, C. H. Yang, J. H. Chen and Y. Chi, *J. Mater. Chem.*, 2007, **17**, 1692–1698.
55 X. H. Zhou, Y. H. Niu, F. Huang, M. S. Liu and A. K. Y. Jen, *Macromolecules*, 2007, **40**, 3015–3020.
56 J. W. Kang, D. S. Lee, H. D. Park, J. W. Kim, W. I. Jeong, Y. S. Park, S. H. Lee, K. Go, J. S. Lee and J. J. Kim, *Org. Electron.*, 2008, **9**, 452–460.
57 J. J. Lin, W. S. Liao, H. J. Huang, F. I. Wu and C. H. Cheng, *Adv. Funct. Mater.*, 2008, **18**, 485–491.
58 Y. Y. Lyu, J. Kwak, O. Kwon, S. H. Lee, D. Kim, C. Lee and K. Char, *Adv. Mater.*, 2008, **20**, 2720–2729.
59 H. C. Yeh, C. H. Chien, P. I. Shih, M. C. Yuan and C. F. Shu, *Macromolecules*, 2008, **41**, 3801–3807.
60 T. Fei, G. Cheng, D. Hu, P. Lu and Y. Ma, *J. Polym. Sci., Part A: Polym. Chem.*, 2009, **47**, 4784–4792.
61 D. Hu, P. Lu, C. Wang, H. Liu, H. Wang, Z. Wang, T. Fei, X. Gu and Y. Ma, *J. Mater. Chem.*, 2009, **19**, 6143–6148.
62 S. Kwon, K. R. Wee, A. L. Kim and S. O. Kang, *J. Phys. Chem. Lett.*, 2009, **1**, 295–299.
63 Y. Y. Lyu, J. Kwak, W. S. Jeon, Y. Byun, H. S. Lee, D. Kim, C. Lee and K. Char, *Adv. Funct. Mater.*, 2009, **19**, 420–427.
64 T. Fei, G. Cheng, D. Hu, W. Dong, P. Lu and Y. Ma, *J. Polym. Sci., Part A: Polym. Chem.*, 2010, **48**, 1859–1865.
65 W. Wei, P. I. Djurovich and M. E. Thompson, *Chem. Mater.*, 2010, **22**, 1724–1731.
66 Y. J. Cho and J. Y. Lee, *J. Phys. Chem. C*, 2011, **115**, 10272–10276.

Open Access Article. Published on 14 augustus 2015. Downloaded on 8/10/2025 15:53:28.
This article is licensed under a Creative Commons Attribution 3.0 Unported Licence.

67 S. O. Jeon, S. E. Jang, H. S. Son and J. Y. Lee, *Adv. Mater.*, 2011, **23**, 1436–1441.
68 K. H. Lee, J. K. Park, J. H. Seo, S. W. Park, Y. S. Kim, Y. K. Kim and S. S. Yoon, *J. Mater. Chem.*, 2011, **21**, 13640–13648.
69 S. Gong, Q. Fu, W. Zeng, C. Zhong, C. Yang, D. Ma and J. Qin, *Chem. Mater.*, 2012, **24**, 3120–3127.
70 D. Hu, G. Cheng, H. Liu, Y. Lv, P. Lu and Y. Ma, *Org. Electron.*, 2012, **13**, 2825–2831.
71 C. W. Lee and J. Y. Lee, *Chem. – Eur. J.*, 2012, **18**, 6457–6461.
72 M. K. Leung, W. H. Yang, C. N. Chuang, J. H. Lee, C. F. Lin, M. K. Wei and Y. H. Liu, *Org. Lett.*, 2012, **14**, 4986–4989.
73 H. Liu, G. Cheng, D. Hu, F. Shen, Y. Lv, G. Sun, B. Yang, P. Lu and Y. Ma, *Adv. Funct. Mater.*, 2012, **22**, 2830–2836.
74 H. Chen, Z. Q. Jiang, C. H. Gao, M. F. Xu, S. C. Dong, L. S. Cui, S. J. Ji and L. S. Liao, *Chem. – Eur. J.*, 2013, **19**, 11791–11797.
75 C. Fan, Y. Chen, Z. Liu, Z. Jiang, C. Zhong, D. Ma, J. Qin and C. Yang, *J. Mater. Chem. C*, 2013, **1**, 463–469.
76 H. Liu, Q. Bai, L. Yao, D. Hu, X. Tang, F. Shen, H. Zhang, Y. Gao, P. Lu, B. Yang and Y. Ma, *Adv. Funct. Mater.*, 2014, **24**, 5881–5888.
77 D. Sun, X. Zhou, H. Li, X. Sun, Y. Zheng, Z. Ren, D. Ma, M. R. Bryce and S. Yan, *J. Mater. Chem. C*, 2014, **2**, 8277–8284.
78 X. Tang, L. Yao, H. Liu, F. Shen, S. Zhang, H. Zhang, P. Lu and Y. Ma, *Chem. – Eur. J.*, 2014, **20**, 7589–7592.
79 Y. Chung, L. Zheng, X. Xing, L. Zhang, M. Bian, L. Xiao, Z. Chen, B. Qu, Q. Gong and J. Kido, *Adv. Electron. Mater.*, 2015, **1**, 140034.
80 D. Liu, M. Du, D. Chen, K. Ye, Z. Zhang, Y. Liu and Y. Wang, *J. Mater. Chem. C*, 2015, **3**, 4394–4401.
81 S. Zhang, Q. L. Xu, Y. M. Jing, X. Liu, G. Z. Lu, X. Liang, Y. X. Zheng and J. L. Zuo, *RSC Adv.*, 2015, **5**, 27235–27241.
82 Q. Zhao, W. Zhang, Z. Fan, J. Li, X. Chen, G. Luo and X. Zhang, *Synth. Met.*, 2015, **204**, 70–75.
83 M. J. Owen, *Ind. Eng. Chem. Prod. Res. Dev.*, 1980, **19**, 97–103.
84 A. Jemmett, *Tribology*, 1968, **1**, 173–177.
85 R. M. Hill, *Silicone Surfactants*, CRC Press, 1999.
86 S. Tadayyon, H. Grandin, K. Griffiths, L. Coatsworth, P. Norton, H. Aziz and Z. Popovic, *Org. Electron.*, 2004, **5**, 199–205.
87 D. Cahen and A. Kahn, *Adv. Mater.*, 2003, **15**, 271–277.
88 C. M. Cardona, W. Li, A. E. Kaifer, D. Stockdale and G. C. Bazan, *Adv. Mater.*, 2011, **23**, 2367–2371.
89 I. G. Hill, A. Kahn, Z. G. Soos and R. A. Pascal, *Chem. Phys. Lett.*, 2000, **327**, 181–188.
90 P. I. Djurovich, E. I. Mayo, S. R. Forrest and M. E. Thompson, *Org. Electron.*, 2009, **10**, 515–520.
91 M. Zhu and C. Yang, *Chem. Soc. Rev.*, 2013, **42**, 4963–4976.
92 S. W. Wen, M. T. Lee and C. H. Chen, *J. Disp. Technol.*, 2005, **1**, 90–99.
93 X. Yang, X. Xu and G. Zhou, *J. Mater. Chem. C*, 2015, **3**, 913–944.
94 S. H. Kim, J. Jang, S. J. Lee and J. Y. Lee, *Thin Solid Films*, 2008, **517**, 722–726.
95 Y. J. Cho, K. S. Yook and J. Y. Lee, *Adv. Mater.*, 2014, **26**, 6642–6646.
96 A. Chaskar, H. F. Chen and K. T. Wong, *Adv. Mater.*, 2011, **23**, 3876–3895.
97 G. Li, L. Wang, H. Ni and C. U. Pittman Jr, *J. Inorg. Organomet. Polym.*, 2001, **11**, 123–154.
98 S. H. Phillips, T. S. Haddad and S. J. Tomczak, *Curr. Opin. Solid State Mater. Sci.*, 2004, **8**, 21–29.

 This journal is © The Royal Society of Chemistry 2015